

DESIGN OF GRID IONIZATION CHAMBERS¹

By O. BUNEMANN,² T. E. CRANSHAW,³ AND J. A. HARVEY⁴

Abstract

Conformal representation theory is applied to a grid ionization chamber having plane parallel electrodes to give formulas useful in design. Expressions are obtained for the inefficiency of grid shielding of the electron collector, the spread of pulse size caused by the induced effect of positive ions, and the proportion of electrons collected by the grid. The theory was verified by experiment. The width of the polonium α -particle line at half-maximum was reduced to 50 kev. or about 1% of the energy by the use of a suitable grid and operating voltages. The corresponding standard deviation from all causes was 22 kev., made up of 2 kev. resulting from induced effect of positive ions, about 17 kev. from noise in the amplifier, and 14 kev. from straggling of ionization, thickness of source, and other effects. The spread caused by positive ions can therefore be almost completely eliminated by a grid.

Introduction

Many experimenters have used the number of ion pairs produced in the track of a charged particle in a gas filled ionization chamber to indicate the initial energy of the particle. The simplest chamber contains two plane parallel electrodes with an electrostatic field applied between them, that is, a high voltage electrode, and a collecting electrode that is connected to a suitable amplifier with a high resistance to ground. When an ionizing particle spends its energy in the gas between the electrodes the ions are collected and a pulse is fed to the amplifier. The rise time of this pulse depends on the orientation of the track in the chamber and the mobility of the components of the ionization, and its decay on the time constant of the capacity and leak resistance of the collecting electrode. This decay is usually arranged to be very long, and a short time constant later in the amplifier determines the output pulse duration. While this is frequently required to be short, the short time constant must be made about 10 times longer than the rise time. This condition is necessary to prevent the variation in rise time due to different track orientations from affecting the output pulse amplitude.

To permit the use of a fast amplifier by speeding up the rate of rise it is necessary first to use as a filling a gas that does not form negative ions by electron attachment, e.g., argon. The negative component of ionization then travels to the collector entirely as electrons, which have a high mobility. However the positive ions, which have a mobility less by a factor of about 1000,

¹ Manuscript received May 28, 1949.

Contribution from the Nuclear Physics and Theoretical Physics Branches, Division of Atomic Energy, National Research Council of Canada, Chalk River, Ontario. Issued as N.R.C. No. 1986. This work first appeared in Report CRP-247, dated May 1, 1946, of the National Research Council of Canada.

² United Kingdom Staff; now at the Atomic Energy Research Establishment, Harwell, England.

³ United Kingdom Staff; now at the Cavendish Laboratory, Cambridge University, Cambridge, England.

⁴ Now at the Massachusetts Institute of Technology, Cambridge, Mass., U.S.A.

induce a charge on the collector of the opposite sign. The potential of the collector will rise rapidly, as the electrons are collected, to an intermediate value given by the collected charge minus the induced charge divided by the capacity, and then rise slowly as the positive ions are removed, to the full potential. The induced charge depends on the orientation of the track in the chamber. If the induction effect of the positive ions can be eliminated the collector will attain its final potential immediately the electrons are collected.

The use of a grid to screen the electron-collecting electrode from the effect of the positive ions was suggested by O. R. Frisch (4). In such a three-electrode chamber the electron pulses are nearly proportional to the ionization in the tracks. The pulse consists of a rapid rise of the order of 1 μ sec., and a fall determined as before. These fast pulses are more easily amplified linearly than those from a two-electrode chamber. A band width can be chosen that is more suitable for reducing the noise level, eliminating microphonics, increasing the permissible counting rate, and decreasing the building up of small background pulses. It is desirable to screen the collecting electrode as effectively as possible and at the same time to avoid the collection of electrons by the screening grid.

The present paper contains a theoretical and experimental study with the purpose of selecting a suitable grid and the proper operating voltages on the electrodes. The success of the arrangement is finally appraised by measuring the "line width" obtainable using a thin α -particle source.

Theoretical Analysis

(a) Preliminary Statement

A grid, G , shown in Fig. 1, is placed in front of the electron-collecting plate P to shield it from fields induced by the positive charges created at Q in the region A to G by ionization of a particle. It is convenient to define the electric field as the *positive* gradient of the potential, with the positive direction of the lines of force accordingly in the direction followed by electrons.

The efficiency of the grid shielding is measured by the extent to which the charge induced on P , or the number of lines per unit area ending there, E_P , is independent of the field E_Q . We define

$$\sigma = \frac{dE_P}{dE_Q}, \text{ for } V_P - V_G = \text{constant}, \quad (1)$$

as the "inefficiency" of the grid, and calculate it as a function of the two geometrical ratios r/d and p/d (Fig. 1). The results are shown by Equation (14) and Fig. 3. The charge induced at P by a unit charge created at Q is then calculated in terms of σ and the distances AQ and AG (Equation (15)).

The proportion of electrons collected by the plate is roughly equal to the proportion of lines that by-pass the grid, as electrons diffuse along the lines of force at the pressures prevailing in an ionization chamber. (This was an initial assumption and is justified by the experimental work.) This proportion

is calculated in terms of the grid geometry and potentials (Fig. 4), and conditions are derived for which all the lines by-pass the grid (Equations (21) and (23)).

(b) *General Method*

For the purpose of calculation it is convenient to replace the grid by a fictitious conducting wall of thickness t held at a potential V'_G that differs from V_G by an amount ΔV depending on E_Q and E_P and the grid geometry (see lower part of Fig. 1).

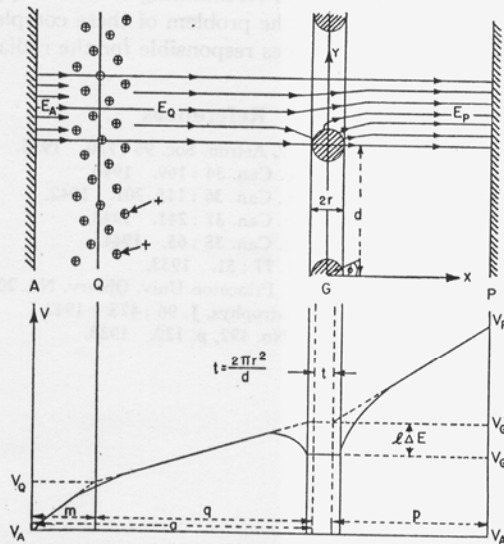


FIG. 1. Field (upper) and potential (lower) in grid ionization chamber. Positive ions and electrons at Q are produced near the cathode A by α -particles. A grid G of parallel wires shields the electron collector P from induced effect of the positive ions.

To calculate t , ΔV , the stagnation points (in the hydrodynamical sense), and numbers of lines, conformal representation theory is used (5). The number of lines passing between the x -axis and a general point in the x - y plane is denoted by U , the potential by V , and an analytic function of $z = x + iy$ is constructed to form the complex quantity $W = U + iV$. The grid wires are simulated by line charges and line dipoles placed along their axes. Nonuniformity of the field is neglected at P and Q . This assumption is permissible when their distances from the grid exceed the pitch of the grid wires.

(c) *Line Charges Induced in Grid Wires*

E_Q lines per unit area arrive at the grid, and E_P lines per unit area leave it. Hence $\Delta E = E_P - E_Q$ lines arise from unit area of grid or $(\Delta E)d$ lines from

a unit length of each wire, implying a line charge density of $(\Delta E)d/4\pi$ units. The complex potential function associated with unit line charge is $2i \log z$, but to represent the array of line charges producing a field periodic in y the function $\sinh \pi z/d$ must be used as argument of the logarithm in place of z . Now the equipotentials derived from the transformation

$$W = 2i \log \sinh \frac{\pi z}{d} \quad (2)$$

are approximately circular in the vicinity of $z = 0, \pm id, \pm 2id$, etc., and the mean value of the potential around an exact circle of radius r (the wire radius) is $2 \log \frac{\pi r}{d}$. Hence the complex potential

$$W_L = \frac{\Delta E}{2\pi} di \left(\log \sinh \frac{\pi z}{d} - \log \frac{\pi r}{d} \right) \quad (3)$$

takes account of the line charges induced in the wires when the grid is at zero potential. For large positive and negative x the potential is given approximately by

$$V_L = \frac{\Delta E}{2} \left(|x| - \frac{d}{\pi} \log \frac{2\pi r}{d} \right) + 0(e^{-2\pi|x|/d}). \quad (4)$$

The deviations from uniformity in the field are therefore small even when $|x|$ is of the same magnitude as d .

(d) *Line Dipoles Induced in Grid Wires*

A uniform field E induces a dipole of intensity $\frac{1}{2}Er^2$ at the center of a cylindrical conductor of radius r . It is reasonable to expect that the dipoles induced in the grid wires have the intensity $\frac{1}{2}\bar{E}r^2$, where $\bar{E} = (E_P + E_Q)/2$ is the mean of the distant fields on the two sides of the grid.

The complex potential function for line dipoles of unit strength, one at each wire position and all orientated in the x direction, is the derivative with respect to z of the unit line-charge function, i.e., $2i(\pi/d) \coth \pi z/d$. In accordance with our expectation, we use as a trial function

$$W_D = -\bar{E}r^2 i(\pi/d) \coth \pi z/d, \quad (5)$$

and show that when combined with the potential function representing the mean field, viz.,

$$W_E = i\bar{E}z, \quad (6)$$

it yields $|z| = r$ as zero equipotential. Neglecting terms of order r^3 ,

$$W_D + W_E = i\bar{E} \left(z - \frac{r^2}{z} \right) = -2\bar{E}r \sin \phi, \quad (7)$$

which is real as required. (The angle ϕ is measured from the x -axis.) Similarly $|z \pm nid| = r$ for $n = 1, 2, \dots$ can be shown to be zero equipotentials.

(e) Complete Potential Function

The combination

$$W = iV_G + W_L + W_D + W_E \tag{8}$$

makes $|z| = r$, $|z \pm nid| = r$ equipotentials with $V = V_G$, and therefore satisfies conditions at the grid. It also yields correct values E_P and E_Q for the field at large positive and negative values of x . The function W yields

$$V = V_G + l(\Delta E) + E_P(x - \frac{1}{2}t) \tag{9}$$

and

$$V = V_G + l(\Delta E) + E_Q(x + \frac{1}{2}t) \tag{10}$$

for large positive and negative values of x respectively. In Equations (9) and (10)

$$l = \frac{d}{2\pi} (\frac{1}{4}\rho^2 - \log \rho), \tag{11}$$

$$t = \frac{d}{2\pi} \rho^2 = \rho r, \tag{12}$$

and

$$\rho = \frac{2\pi r}{d}. \tag{13}$$

More exact analysis reveals additional even powers of ρ in the formulas for l and t , beginning with

$$-\frac{7}{288} \left(\frac{d}{2\pi}\right) \rho^4 \quad \text{and} \quad -\frac{1}{12} \left(\frac{d}{2\pi}\right) \rho^4 \quad \text{respectively.}$$

These terms enter when, in order to make the equipotentials at the wires more nearly circular, quadrupoles are considered. The ratio l/d is plotted as a function of r/d in Fig. 2.

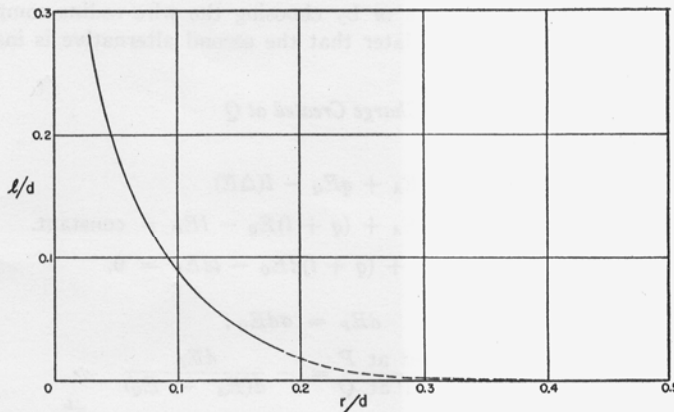


FIG. 2. Curve of l/d as a function of r/d , which is convenient for calculating the inefficiency τ of a grid.

(f) *Inefficiency of Shielding*

The inefficiency σ can be obtained by differentiating the relation

$$V_P - V_G = pE_P + l(\Delta E) = (p + l)E_P - lE_Q = \text{constant},$$

giving

$$\sigma = \frac{dE_P}{dE_Q} = \frac{l}{p + l} \approx \frac{d}{2\pi p} \log \left(\frac{d}{2\pi r} \right). \quad (14)$$

Curves of constant σ are shown in Fig. 3. It is seen that σ can be made small and the grid efficient either by choosing a grid-to-collector distance

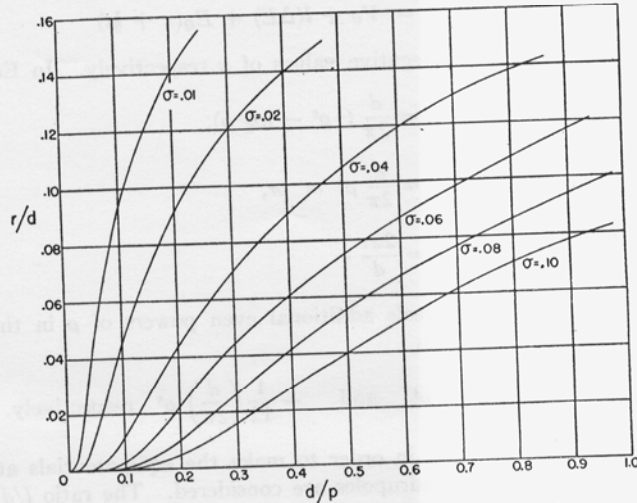


FIG. 3. Curves of constant inefficiencies σ of grids.

large compared to the pitch or by choosing the wire radius comparable to the pitch. It will be seen later that the second alternative is inadmissible (Equation (23)).

(g) *Charge Induced at P by Charge Created at Q*

From Fig. 1

$$\begin{aligned} V_G - V_A &= mE_A + qE_Q - l(\Delta E) \\ &= mE_A + (q + l)E_Q - lE_P = \text{constant}. \end{aligned}$$

Therefore

$$mdE_A + (q + l)dE_Q - ldE_P = 0,$$

which with the relation

$$dE_P = \sigma dE_Q,$$

yields

$$\begin{aligned} \frac{\text{charge induced at } P}{\text{charge created at } Q} &= - \frac{dE_P}{d(E_A - E_Q)} \\ &= \frac{\sigma m}{a + l(1 - \sigma)} \approx \sigma \frac{\bar{A}Q}{\bar{A}G}. \end{aligned} \quad (15)$$

(h) *Fraction of Lines Intercepted by Grid*

The real part U of the function W can be used to determine the number of lines leaving Q that are intercepted by the grid. On the grid wire where $|z| = r$ we obtain

$$U = -\phi(\Delta E) \frac{d}{2\pi} - 2\bar{E}r \sin \phi. \quad (16)$$

The stagnation points (5, p. 108), i.e., the points on the circumference where lines cease to enter and instead leave the grid, occur where U is stationary,

$$\text{i.e.,} \quad \frac{\partial U}{\partial \phi} = 0.$$

Therefore

$$\cos \phi = -\frac{(\Delta E)}{2\bar{E}} \frac{d}{2\pi r} = -\frac{(\Delta E)}{2\rho\bar{E}}. \quad (17)$$

The number of lines collected by each wire from the field E_Q is given by the difference of U between the two solutions of (17) going via $\phi = \pi$. This difference is

$$\begin{aligned} \Delta U &= 4\bar{E}r |\sin \phi| - 2|\pi - \phi| (\Delta E) \frac{d}{2\pi} \\ &= 4\bar{E}r \sqrt{1 - \left(\frac{\Delta E}{2\bar{E}\rho}\right)^2} - 2(\Delta E) \frac{d}{2\pi} \cos^{-1} \left(\frac{\Delta E}{2\bar{E}\rho}\right). \end{aligned} \quad (18)$$

The number of lines collected by unit area of the grid is $\Delta U/d$, and the ratio between this and E_Q represents the grid loss λ :

$$\lambda = \frac{\Delta U}{E_Q d} = \frac{E_P - E_Q}{\pi E_Q} \left\{ \sqrt{\left(\frac{E_P + E_Q}{E_P - E_Q} \rho\right)^2 - 1} - \cos^{-1} \left(\frac{E_P - E_Q}{E_P + E_Q} \frac{1}{\rho}\right) \right\}. \quad (19)$$

The proportion of lines that end on the collector rather than the grid, $1 - \lambda$, is plotted as a function of E_P/E_Q for three values of ρ in Fig. 4 over the range where the square root and the inverse cosine are real, viz.,

$$\frac{1 - \rho}{1 + \rho} < \frac{E_P}{E_Q} < \frac{1 + \rho}{1 - \rho}. \quad (20)$$

The ends of the interval correspond to the conditions where the stagnation points unite and slip off the wires in the direction of the weaker field. For

$$\frac{E_P}{E_Q} > \frac{1 + \rho}{1 - \rho} \quad (21)$$

all lines by-pass the grid, and $1 - \lambda = 1$. For

$$\frac{E_P}{E_Q} < \frac{1 - \rho}{1 + \rho} \quad (22)$$

all of the balance between E_Q and E_P is collected by the grid,

$$\lambda = \frac{E_Q - E_P}{E_Q} \quad \text{and} \quad 1 - \lambda = \frac{E_P}{E_Q}.$$

Since V'_G differs from V_G , E_P/E_Q is not strictly proportional to the grid-plate potential difference for fixed $V_G - V_A$. Deviations from proportionality are of the order of σ . In particular zero grid-collector potential difference corresponds to $E_P/E_Q = \sigma$. The origin must be shifted to the right by an amount σ in Fig. 4 if the abscissa is to become a more accurate measure of the grid-collector potential difference (broken line).

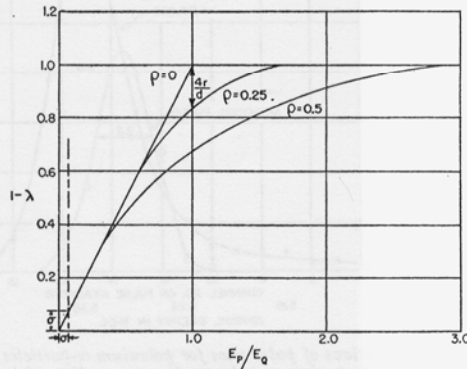


FIG. 4. Fraction of lines from cathode that end on electron collector is plotted against the field ratio E_P/E_Q . The origin must be shifted by σ if $(V_P - V_G)/p$ is used for E_P . ($\rho = 2\pi r/d$).

(i) Condition on Potential Differences for Zero Grid Interception

Condition (21) applies when all lines by-pass the grid. If this condition is satisfied in the absence of positive charge at Q , then it will certainly be satisfied in the presence of such charge. Hence a sufficient condition on V_A , V_P , and V_G can be derived on the assumption that there is no charge at Q . Substitution for E_P and E_Q then gives the condition:

$$\frac{V_P - V_G}{V_G - V_A} \geq \frac{p + p\rho + 2l\rho}{a - a\rho - 2l\rho}. \quad (23)$$

This must be balanced against the condition that σ (or l/p) should be small for efficient shielding (Equation (14)).

Experimental Investigation

An experimental investigation was undertaken to test the main results from the theoretical analysis and to indicate what lower limit in width of an α -particle line might be realized in practice.

(a) Ionization Chamber

The ionization chamber consisted of two parallel plates, 10 cm. square and about 6 cm. apart, mounted on insulators inside a cylindrical vessel. The

gas was argon, usually at a pressure of 3 atm. A grid of parallel wires could be mounted 1.43 or 0.67 cm. in front of the collector. Two grids were tested; one consisted of No. 38 copper wires 0.20 cm. apart, and the other of No. 36 copper wires 0.091 cm. apart. A negative potential of 1200 v. was applied to the cathode, which produced an adequate field between the electrodes for electron collection.

Sources of α -particles were made by evaporating a solution of polonium 210 on gold foils. The source, covered by a collimator consisting of $\frac{1}{8}$ in. holes in a $\frac{1}{32}$ in. aluminum sheet, was placed against the cathode. Without the collimator the distribution of pulse sizes was not symmetrical about the maximum and had a tail on the low energy side. This distortion is attributed to α -particles that had traveled approximately in the plane of the source and lost energy in irregularities in the source or in the backing foil before being scattered into the gas.

The electronic equipment for the measurement of pulse size has been described (1). The ionization pulses at the collector were fed into an amplifier designed for low noise and high stability of gain and then into a cutoff amplifier that subtracted a predetermined voltage and amplified the remainder. The output pulses were electronically sorted into groups according to height by a pulse analyzer (3). In this way the "line" containing the pulse heights could be expanded to show its shape and thereby to yield quantitative information on width at half-maximum or alternatively on the standard deviation from the mean.

(b) Collection of Electrons by the Grid

The first point considered was the possible collection of electrons by the grid. This is undesirable for two reasons. (1) The pulse size and the signal-to-noise ratio would be reduced. (2) The fraction of electrons collected might depend somewhat on the track orientation, and thus an additional cause of spread might enter.

Fig. 4 shows the fraction of lines from the cathode which by-pass the grid and end on the collecting electrode. If the electrons diffuse along the lines of force these relations also give the fractions of charge reaching the collecting electrode. Fig. 5 shows two curves of observed pulse size plotted against the ratio of the fields on the two sides of the grid. Figs. 4 and 5 are in good agreement, particularly at the upper end. For this region the field lines are nearly straight in the chamber. For very low potential difference between grid and collector the field lines have considerable curvature, and agreement is not as good. The pulses are larger than those calculated; this suggests that electrons slip off the field lines and reach the collector. The intercept for zero potential difference between grid and collector is greater than σ . It is seen

in Fig. 5 that a voltage can be chosen for the grid at which it does not collect electrons. The chamber is ordinarily operated under this condition.

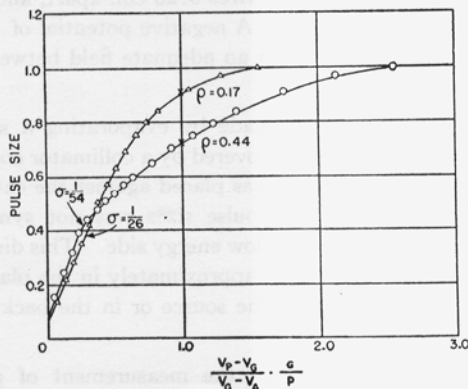


FIG. 5. Observed pulse size, indicating fraction of electrons reaching the collector, is plotted against $\frac{V_p - V_g}{V_g - V_a} \cdot \frac{a}{p}$ (Grids Nos. 2 and 3). The two points marked by crosses were calculated from theory.

(c) Spread of Pulse Size

Table I and Fig. 6 show the results of a typical run with polonium α -particles. The distribution of pulses from a signal generator is included. The distribution of the α -particle pulses is approximately Gaussian having a standard deviation s_1 . Five causes of spread may be noted: (1) thickness of source

TABLE I
PULSE DISTRIBUTIONS FOR α -PARTICLES AND ARTIFICIAL SIGNALS

Pulse analyzer channel No.	α -particles, counts	Artificial pulses, counts
1	0	—
2	2	—
3	2	—
4	2	—
5	4	—
6	4	—
7	8	—
8	8	—
9	8	—
10	10	2
11	20	10
12	48	96
13	64	158
14	116	162
15	124	66
16	116	20
17	48	—
18	14	—
19	2	—

material, (2) straggling of ionization, (3) variation of rise time of the electron pulses, (4) noise of the amplifier, and (5) induced effect of positive ions, as described in the introduction. The last item will be referred to as spread

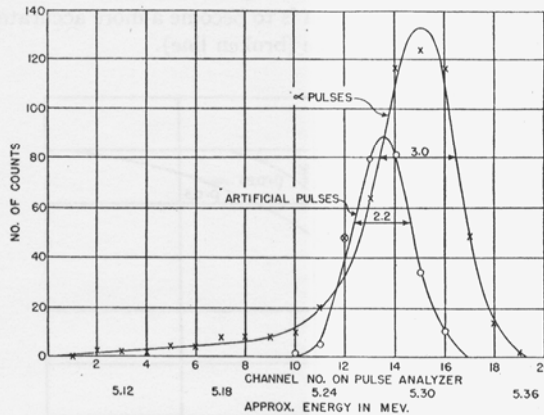


FIG. 6. Typical distributions of pulse sizes for polonium α -particles and artificial pulses (Grid No. 1). One channel spacing on pulse analyzer is equal to 15 kev.

caused by the chamber. The observed standard deviation s_1 is assumed to be associated with the separate standard deviations $s_s, s_i, s_r, s_n,$ and s_e from the above causes respectively by the formula:

$$s_1 = \sqrt{s_s^2 + s_i^2 + s_r^2 + s_n^2 + s_e^2}.$$

In the present experiments $s_s, s_i,$ and s_r always occur together, while s_n can be obtained by using artificial pulses. It is intended to compare the values of s_e obtained from measurements with the various grids with the theory.

(d) Spread of Pulse Size Due to Chamber

The distribution of pulse size will be examined, the effect of orientation of the α -particle track being taken into account. Noting that the induced effect of the positive ions depends on the first power of m (Equation (15)), the idea of center of ionization may be introduced (similar to center of mass in mechanics). The effective range \bar{R} , measured from the source of the α -particle to the center of ionization in the track, is evaluated from the Bragg curve for a single polonium α -particle. The perpendicular distance from the center of ionization to the cathode may be taken as the value of m .

The centers of ionization possess a distribution of m 's for a point source of α -particles at O in Fig. 7, without a collimator, having limits zero and \bar{R} . If N α -particles are emitted isotropically, the number making angles between θ and $\theta + d\theta$ with the normal is

$$\frac{2\pi N \bar{R}^2 \sin \theta d\theta}{4\pi \bar{R}^2} = \frac{N}{2} \sin \theta d\theta = \frac{N dm}{2\bar{R}}.$$

Thus, the distribution of m 's is rectangular (extending from $m = 0$ to $m = \bar{R}$), giving a similar distribution of pulse sizes. The maximum pulse size is that for which $m = 0$ and the minimum is that for which $m = \bar{R}$. In the absence of a

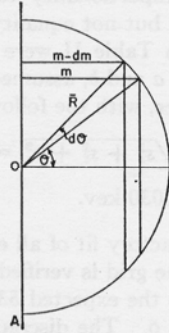


FIG. 7. Source at point O emits α -particles of effective range \bar{R} measured from O to centers of ionization in tracks.

grid the fractional width of the pulse distribution is equal to \bar{R} /(separation of electrodes). Fig. 8 shows pulse distributions observed without a grid. The

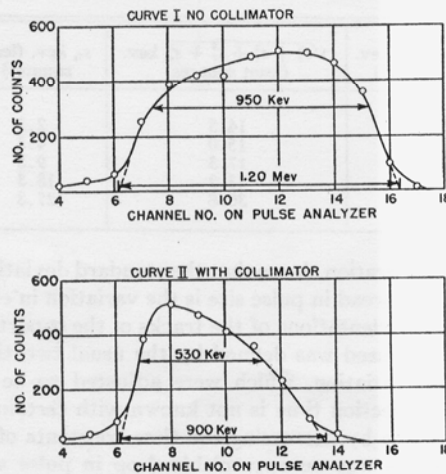


FIG. 8. Observed distributions of α -particle pulses in ionization chamber without a grid. Separation of electrodes was 5.9 cm. Argon pressure was 2 atm. Effect of collimator is shown.

effective range \bar{R} was calculated to be 1.15 cm. in argon at 2 atm., and the separation of electrodes was 5.9 cm. Thus the expected width of the pulse distribution of polonium α -particles without a collimator is $\frac{1.15}{5.9} \times 5.30$ Mev. = 1.0 Mev., in fair agreement with that observed (Curve I, Fig. 8).

When a collimator is used the distribution of pulse size is changed, as shown in Fig. 8. The collimator cuts off the largest pulses, which must come from the tracks making small angles with the cathode, since the induced effect of the positive ions is least for these tracks. The width at 60.7% of the maximum is reduced by the factor $950/530 = 1.8$. The calculated reduction is about 2.5. Since neither distribution is Gaussian, the first being rectangular, and the second nearly triangular, the exact value chosen for the effect of the collimator is rather arbitrary. The standard deviation when the collimator is present is about $\frac{1}{2}$ (530) kev. This may be related to the energy 5.30 Mev. of the polonium α -particle as follows:

$$\text{Standard deviation} = \frac{1}{2} \left(\frac{\bar{R}}{5.9f} \right) 5300 \text{ kev.} = \frac{1}{2} (530) \text{ kev.,}$$

where f is the collimator factor. Using $\bar{R} = 1.15$ cm. it is found that $f = 2.0$. It will be seen later that with a good grid shielding the collector the spread due to the chamber is not as large as other spreads. Therefore the distribution of pulse size with a spread due only to the chamber may be assumed Gaussian, and the collimator factor 2.0 carried over into the corresponding standard deviation.

(e) *Shielding by the Grid*

The standard deviation of a pulse distribution was estimated by three methods (6, pp. 134-153). (1) The width of the peak was measured at 60.7% of the maximum. (2) The mean square deviation was obtained from the histogram and Sheppard's correction applied. (3) An ogive plot, such as shown in Fig. 9, was used. The last method appeared most reliable. For

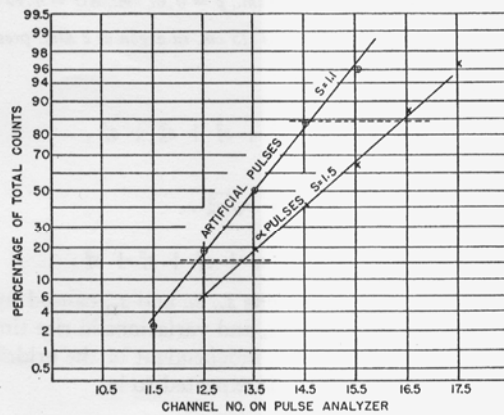


FIG. 9. Ogive plot for estimating standard deviation of a pulse distribution. Standard deviation is half of number of channels between intersections at dotted lines.

the data in Table I the standard deviations are 1.5 and 1.1 channel widths of the pulse analyzer respectively for the α -particles and artificial pulses.

Table II summarizes the experimental results for four different grid arrangements. The inefficiencies σ were calculated from Equation (14). The standard deviations are the averages of five determinations in each case. The small variations in s_n observed for the different experimental arrangements are in approximate agreement with the expected effects of changing the capacity of the chamber.

TABLE II
STANDARD DEVIATIONS IN PULSE DISTRIBUTIONS

s_1 = standard deviation for α -particle pulses
 s_2 = standard deviation for artificial pulses
1 channel spacing = 15 kev.

Grid No.	$\sigma \times 10^3$	s_1 , channels	s_2 , channels	$\sqrt{s_1^2 - s_2^2}$, channels	$\sqrt{s_1^2 - s_2^2}$, kev.
1	8.73	1.42	1.08	0.92	13.8
2	18.5	1.66	1.25	1.09	16.4
3	38.3	1.65	1.05	1.27	19.1
4	78.4	1.74	1.10	1.35	20.2
4a	78.4	2.40	1.10	2.13	32.0

Grid No. 1: $r = 6.35 \times 10^{-3}$ cm., $d = 0.091$ cm., $p = 1.43$ cm., $AG = 4.49$ cm., $\bar{R} = 0.77$ cm. (argon at 3 atm. pressure).

Grid No. 2: $r = 6.35 \times 10^{-3}$ cm., $d = 0.091$ cm., $p = 0.67$ cm., $AG = 4.93$ cm., $\bar{R} = 0.77$ cm.

Grid No. 3: $r = 5.34 \times 10^{-3}$ cm. (wire coated with Aquadag), $d = 0.20$ cm., $p = 1.43$ cm., $AG = 4.49$ cm., $\bar{R} = 0.77$ cm.

Grid No. 4: $r = 5.34 \times 10^{-3}$ cm., $d = 0.20$ cm., $p = 0.67$ cm., $AG = 4.93$ cm., $\bar{R} = 0.77$ cm.

Grid No. 4a: same as No. 4 except that $\bar{R} = 1.15$ cm. in argon at 2 atm. pressure.

For the α -particle pulses

$$s_1 = \sqrt{s_s^2 + s_i^2 + s_r^2 + s_n^2 + s_c^2},$$

and for the artificial pulses

$$s_2 = \sqrt{s_n^2}.$$

Therefore

$$\sqrt{s_1^2 - s_2^2} = \sqrt{s_s^2 + s_i^2 + s_r^2 + s_c^2}.$$

The squares of the standard deviations s_s , s_i , and s_r , caused by the thickness of the source, straggling of ionization, and variations in rise time, should form an approximately constant quantity, independent of the grid. The standard deviation s_c caused by the chamber is expected to be

$$s_c = \frac{\sigma \bar{R}}{2f(a + l(1 - \sigma))} 5300 \text{ kev.} = \eta \times 5300 \text{ kev.}$$

from Equation (15) and the effect of the collimator. Owing to the finite extent of the electrodes and the proximity of the wall of the surrounding vessel one might expect s_e to be merely proportional to this expression. Although the constant of proportionality turned out to be approximately unity, at first proportionality but not equality was assumed. The measured quantities $\sqrt{s_1^2 - s_2^2}$ given in Table II were set equal to $\sqrt{a + b\eta^2}$. The best values of the parameters a and b , assumed to be constants, were obtained by the method of least squares, with the following result:

$$\sqrt{a} = \sqrt{s_e^2 + s_i^2 + s_r^2} = 14.3 \text{ kev.}$$

and

$$\sqrt{b} = 6030 \text{ kev.}$$

Table III shows that a satisfactory fit of all experimental data was obtained. The predicted shielding by the grid is verified, as shown by $\sqrt{b} = 6030$ kev. being approximately equal to the expected 5300 kev. or alternatively by the agreement of Columns 5 and 6. The discrepancy involves f directly, which is difficult to estimate owing to the asymmetry of the pulse distribution, as pointed out above.

TABLE III
STANDARD DEVIATIONS CAUSED BY CHAMBER

Grid No.	$\eta \times 10^4$	$\sqrt{s_1^2 - s_2^2}$, kev. (observed)	$\sqrt{s_e^2 + s_i^2 + s_r^2 + s_c^2}$, kev. (least squares)	s_e , kev. (least squares)	$\eta \times 5300$ kev. (theory)
1	3.74	13.8	14.5	2.2	2.0
2	7.19	16.4	15.0	4.3	3.8
3	16.25	19.1	17.3	9.8	8.6
4	30.3	20.2	23.2	18.3	16.1
4a	45.3	32.0	30.8	27.3	24.0

The following consideration shows that the standard deviation s_r is relatively small. This cause of spread in pulse size is the variation in electron collection times due to different orientations of the tracks of the α -particles. The band width of the amplifier used was defined by the usual two time constants of smoothing and differentiation, which were adjusted to be 5 and 50 μ sec. respectively. The collection time is not known with certainty, but a rough measurement was made by decreasing the time constants of the amplifier to 1 and 10 μ sec. There was no appreciable drop in pulse amplitude, which indicates a collection time of about 1 μ sec. With time constants of 5 and 50 μ sec. a variation in collection time between zero and 2 μ sec. would introduce a total spread of only 4 kev., which is much smaller than the spreads introduced by source thickness and ionization straggling.

(f) *Limitations on Standard Deviations*

The standard deviation from all causes on the pulse distribution of polonium α -particles was found to be as low as 22 kev. when a suitable grid was placed

in front of the electron collector. The corresponding width of the line at half-maximum was 50 kev. or about 1% of the energy of the polonium α -particle. The standard deviation caused by the induced effect of the positive ions was found to be as low as 2 kev. when a carefully designed grid was used to shield the collector. This cause of spread is now negligible, and further decrease in line width can be effected only by attention to other causes.

Through the use of artificial pulses the standard deviation caused by noise in the head amplifier was found to be about 17 kev. With existing tubes not much improvement can be expected here. The standard deviation caused by thickness of source, straggling of ionization, and variations in rise time of the pulses was 14 kev. From Fano's theory (2) an estimate of the standard deviation caused by straggling of ionization is about 8 kev. With the best conditions an over-all standard deviation of about 18 kev. may perhaps be attained. This corresponds to a width of 45 kev. at half-maximum for the polonium α -particle line.

Acknowledgments

We wish to thank Dr. B. W. Sargent and Mr. G. C. Hanna for their assistance and criticisms in preparing this paper for publication.

References

1. CRANSHAW, T. E. and HARVEY, J. A. Can. J. Research, A, 26 : 243. 1948.
2. FANO, U. Phys. Rev. 72 : 26. 1947.
3. FREUNDLICH, H. F., HINCKS, E. P., and OZEROFF, W. J. Rev. Sci. Instruments, 18 : 90. 1947.
4. FRISCH, O. R. Unpublished report, BR-49. Isotope analysis of uranium samples by means of their α -ray groups. British Atomic Energy Project.
5. SHOTTKY, W. (Part IIA) and POHLHAUSEN, K. (Part IIB). Theory of functions as applied to engineering problems. Edited by R. Rothe, F. Ollendorff, and K. Pohlhausen. Technology Press, Massachusetts Institute of Technology, Cambridge, Mass., U.S.A.
6. YULE, G. U. and KENDALL, M. G. An introduction to the theory of statistics. Charles Griffin & Co. Ltd., London, England. 1940.